Journal of Physical Science, Vol. 34(3), 21–36, 2023

The Kinetic Behaviour of Mn^{+7}/H^{+} Ions Towards Mannose Molecule

Mustafa Jaip Allah Abdelmageed Abualreish

[1]Northern Border University, Faculty of Science, Department of Chemistry, 91451-2251, Arar, Kingdom of Saudi Arabia

Corresponding author: mustjeed_2008@hotmail.com

Published Online: 6 December 2023

To cite this article: Abualreish, M. J. A. (2023). The kinetic behaviour of Mn^{+7}/H^{+} ions towards mannose molecule. *J. Phys. Sci.*, 34(3), 21–36. https://doi.org/10.21315/jps2023.34.3.2

To link to this article: https://doi.org/10.21315/jps2023.34.3.2

ABSTRACT: *The spectrophotometric method monitored the uncatalysed redox reaction between Mn^{+7}/H^{+} ions and mannose sugar molecules kinetically at constant ionic strength maintained using potassium nitrate (KNO_3). The kinetic study showed that the reaction was pseudo-first order concerning Mn^{+7} and mannose, and the rate of reaction increases by increasing the concentration of Mn^{+7}, mannose and H^{+} and increasing temperature. The reaction rate was enhanced by 3×10^{-4}m of Mn^{+7} concentration, and the oxidation with Mn^{+7} was faster using 2×10^{-2}m of mannose and 5×10^{-1}m of H^{+}. The temperature dependence was carried out under fixed experimental conditions, from which the activation energy of the reaction (E_a) in KJ.mol^{-1} was found to be 61.1, and the frequency factor (A) in sec^{-1} was 10.52×10^{5} other physical functions, namely, the free energy change (ΔG) in KJ.mol^{-1} and the entropy change (ΔS) in J.K^{-1} were also calculated at different temperatures. Qualitative analysis of the reaction products revealed the formation of formic acid. A rate law was derived from the proposed mechanism, which agreed well with experimental kinetics.*

Keywords: spectrophotometry, manganese(vii), mannose, qualitative analysis, physical functions

1. INTRODUCTION

Carbohydrates are an essential energy source for the various metabolic activities of living organisms, the energy released by their oxidation.[1] The oxidation of various sugars has been carried out using transition metal ions,[2] inorganic acids,[3] organometallic complexes[4] and enzymes.[5] These were exposed to various

reaction settings, including the effects of pH, temperature, ionic strength, oxidant and substrate concentrations.[6,7] To examine carbohydrates biochemical and physiochemical characteristics and reactivities, mainly mono- and di-saccharides, were highly dependable on the biological and economic of the carbohydrates.[2,8,9] Chemistry has been substantially improved by studying carbohydrates and their derivatives, particularly when understanding how molecule shape and conformation play a part in chemical processes.[10] In both acidic and alkaline conditions, the kinetics of the oxidation of sugars by various oxidising agents has been studied.[11,12]

Potassium permanganate ($KMnO_4$) is one of the most versatile oxidising agents used to oxidise various compounds such as sugars.[13,14] For example, $KMnO_4$ oxidises alkenes and aldehydes to carboxylic acids under acidic conditions.[9]

Rarely is the oxidation of sugars carried out using the oxidation potential of $KMnO_4$ as an oxidant. On the contrary, almost all uses of $KMnO_4$ take advantage of its oxidising capabilities since, although being a powerful oxidising agent, it does not create harmful by-products, and there are only a few publications addressing the oxidation of sugars.

This study is significant since there has not been any prior research on the oxidation of sugars in an acid media that involves isolating the oxidised chemical and using cutting-edge methods to understand its mechanism and structure.

The present work aimed to investigate the uncatalysed redox reaction between Mn^{+7}/H^{+} ions and mannose sugar molecules at constant ionic strength, explore the kinetic behaviour, and propose a mechanism and rate law to explain the reaction process.

2. EXPERIMENTAL

2.1 Reagents

All materials were supplied by Scarlab. S.L (Spain), Acrös (USA) and Nice (India) companies. Laboratory grade $KMnO_4$ (99%–100%) and sulfuric acid (H_2SO_4) (95%–98%) were obtained from Scarlab. S.L. D(+)mannose(99%) was obtained from Acrös and potassium nitrate (KNO_3) (99%) was obtained from Nice. All solutions were prepared according to standard analytical procedures.

2.2 Methods

To investigate the influence of Mn^{+7}, H_2SO_4, KNO_3 and mannose on the uncatalysed redox reaction between Mn^{+7}/H^+ ions and mannose-sugar molecule, all kinetic runs were performed at room temperature, and deionised water was used.

The temperature range of 30°C to 50°C was utilised to examine the impact of temperature on the uncatalysed redox reaction between Mn^{+7}/H^+ ions and the mannose sugar molecule. All experiments in the current study were carried out by monitoring the change in absorbance of Mn^{+7} with respect to time utilising a Jasco Model V570 UV/VIS spectrophotometer (180 nm –1100 nm) in conjunction with an accessory PAC-743/743R automated 6/8-1 position peltier cell changer (water-cooled) temperature controller. To determine the maximum absorption wavelength, the Mn^{+7} absorption spectra was also obtained in an aqueous solution.[16]

2.2.1 Stoichiometry

Different [Mn^{+7}]: [mannose] ratios were equilibrated for 72 h at room temperature, with the [Mn^{+7}] condition much greater than [mannose], and the residual amount of [Mn^{+7}] in different sets was estimated.[17]

2.2.2 Qualitative product analysis

The literature has reported that when $KMnO_4$ reacts with hydrogen sulphate, the following reaction takes place.[18]

$$2KMnO_4 + 3H_2SO_4 \rightarrow K_2SO_4 + 2MnSO_4 + 5[O] + 3H_2O$$

The oxygen produced by the reaction reacts with the sugar to form the corresponding acid. Hence,

$$RCHO + [O] \rightarrow RCOOH$$

The presence of formic acid was confirmed by adding 1,8-dihydro naphthalene-3,6-disulfonic acid (Chromotropic acid) to various reaction mixtures of Mn^{+7} and mannose.

2.2.3 Influence of [Mn^{+7}]

The reaction was examined at various beginning concentrations to gauge the impact of Mn^{+7} concentration on the oxidation rate of Mn^{+7} in the range of 1–5 × 10^{-4} m. Mannose, H_2SO_4 and KNO_3 concentrations were maintained at 2 × 10^{-2} m, 1 × 10^{-1} m and 3 × 10^{-1}m, respectively. The temperature was kept

constant at 303°K. The reaction was monitored by observing the change in the optical density of Mn^{+7} in the reaction mixture at λ_{max} 545 nm. The absorbance was recorded after every 60 s.

2.2.4 Influence of [mannose]

In various concentrations 1–5 × 10^{-2} m, the impact of mannose concentration was investigated. The concentrations of Mn^{+7}, H_2SO_4 and KNO_3 were kept constant at 1 × 10^{-4} m , 1 × 10^{-1} m and 3 × 10^{-1} m, respectively. The temperature was kept constant at 303°K.

2.2.5 Influence of [H_2SO_4]

By varying the H_2SO_4 concentration (1–5) × 10^{-1} m at a constant concentration of mannose (2 × 10^{-2} m), Mn^{+7} (1 × 10^{-4} m), KNO_3 (3 × 10^{-1} m) and a temperature of 303°K, the effect of hydrogen ion concentration was investigated.

2.2.6 Influence of temperature

Temperature dependence was investigated by keeping the concentration of Mn^{+7} constant at 1 × 10^{-4} m, mannose at 2 × 10^{-2} m, H_2SO_4 at 1 × 10^{-1} m and KNO_3 at 3 × 10^{-1} m, while the temperature varied from 303°K–323°K. According to the literature, the activation energy (E_a) and other thermodynamic characteristics were assessed.[19]

2.3 Mechanism and Rate Law of the Reaction

It was found that the stable reduction product of $KMnO_4$ in an acidic medium is the manganate ion [Mn^{+7}]. Mannose interacts with the permanganate ion [Mn^{+7}] to generate a complex. In the eventual presence of a nucleophile, this complex transforms into the aldonic acid.[20]

3. RESULTS AND DISCUSSION

The maximum absorption wavelength was determined by recording the Mn^{+7} absorption spectra in an aqueous solution. Two maxima can be seen in the spectra at 525 nm and 545 nm, respectively (Figure 1). Therefore, 545 nm was used as λ_{max}.

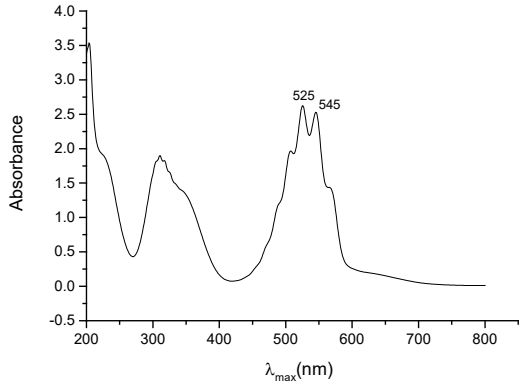

Figure 1: The maximum absorption(λ_{max}) for Mn^{+7}.

3.1 Stoichiometry

The stoichiometry of the uncatalysed reaction studied in this investigation showed that one mole of mannose consumes two moles of Mn^{+7}, so the following stoichiometric equations could be formulated:

$$\underset{\text{Mannose}}{C_6H_{12}O_6} + 2MnO_4^- \xrightarrow{H^+} \underset{\text{Arabinonic acid}}{C_5H_{10}O_5} + \underset{\text{Formic acid}}{HCOOH} + 2MnO_3^-$$

3.2 Product Qualitative Analysis

The oxygen produced by the reaction reacts with the sugar to create the corresponding acid. Hence,

$$RCHO + [O] \longrightarrow RCOOH$$

The appearance of a purplish-pink colour confirmed the presence of formic acid.

3.3 Kinetic Measurements

3.3.1 Influence of [Mn^{+7}] on the redox reaction

Absorbance was determined after every 60 s (Table 1). The values of rate constants (Table 3) were obtained from the curve of ln A_o-A_∞/A_t-A_∞ versus time (Table 2, Figure 2). These findings demonstrate that for Mn^{+7}, the reaction displays first-order kinetics.

Table 1: Influence of [Mn^{+7}] on the redox reaction.

t	1×10^{-4} m	2×10^{-4} m	3×10^{-4} m	4×10^{-4} m	5×10^{-4} m
0	0.0792	0.4607	0.7199	0.8883	0.0821
60	0.0642	0.4336	0.6511	0.8816	0.0817
120	0.0621	0.4299	0.6506	0.8744	0.0794
180	0.056	0.4205	0.6476	0.8726	0.0768
240	0.0468	0.4198	0.6461	0.8704	0.0756
300	0.0453	0.4141	0.6437	0.8667	0.0729
600	0.0442	0.4014	0.6422	0.8641	0.0709

Table 2: The values of $\ln A_o\text{-}A_\infty/A_t\text{-}A_\infty$ of the redox reaction at various Mn^{+7} concentration.

ln Ao–A∞/At–A∞	1×10^{-4} m	2×10^{-4} m	3×10^{-4} m	4×10^{-4} m	5×10^{-4} m
$\ln(A_0–A_{600}/A_{60}–A_{600})$	0.559615788	0.610642853	2.166803981	0.324151752	0.036367644
$\ln(A_0–A_{600}/A120–A_{600})$	0.670547349	0.732705219	2.224623552	0.854208738	0.275847615
$\ln(A_0–A_{600}/A_{180}–A_{600})$	1.08724853	1.132920971	2.666456304	1.04628647	0.640961427
$\ln(A_0–A_{600}/A_{240}–A_{600})$	2.599836616	1.170258641	2.991878704	1.34580300	0.86835127
$\ln(A_0–A_{600}/A_{300}–A_{600})$	3.460037882	1.541007313	3.947390149	2.230841188	1.722766598

Note: $A_{600} = A_{\infty}$

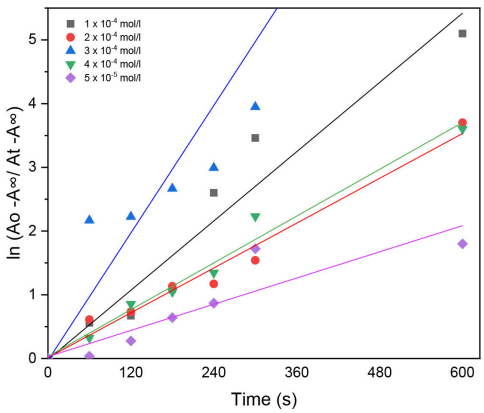

Figure 2: Influence of [Mn^{+7}] on the redox reaction.

Table 3: Values of the rate constants of the redox reaction at different Mn^{+7} concentrations.

Concentration of Mn^{+7} at mol/l	1×10^{-4}	2×10^{-4}	3×10^{-4}	4×10^{-4}	5×10^{-4}
The slope = k	0.00906	0.00586	0.01668	0.00612	0.00343

3.3.2 Influence of [mannose]

Absorbance was determined after every 60 s (Table 4). The rate constants values (Table 6) were determined from the slope curve of ln Ao-A∞/At-A∞ versus time (Table 5, Figure 3). These results show that the reaction rate increases with increasing mannose concentration, suggesting that the reaction exhibits first-order kinetics concerning mannose.

Table 4: Influence of [mannose] on the redox reaction.

t	1×10^{-2} m	2×10^{-2} m	3×10^{-2} m	4×10^{-2} m	5×10^{-2} m
0	0.2395	0.1786	0.2203	0.2196	0.2455
60	0.2351	0.1764	0.2104	0.2150	0.2408
120	0.2324	0.1734	0.2072	0.2035	0.2381
180	0.2253	0.1721	0.2065	0.2005	0.2356
240	0.2186	0.1705	0.2057	0.2000	0.2236
300	0.2059	0.1685	0.2024	0.1970	0.2217
600	0.1832	0.1677	0.1975	0.1734	0.2057

Table 5: The values of ln Ao-A∞/At-A∞ of the redox reaction at various mannose concentration.

ln Ao-A∞/At-A∞	1×10^{-2} m	2×10^{-2} m	3×10^{-2} m	4×10^{-2} m	5×10^{-2} m
$\ln(A_0-A_{600}/A_{60}-A_{600})$	0.081375745	0.225439764	0.569533225	0.104879631	0.12566578
$\ln(A_0-A_{600}/A_{120}-A_{600})$	0.134800912	0.648296614	0.854634650	0.428454626	0.20570849
$\ln(A_0-A_{600}/A_{180}-A_{600})$	0.290646794	0.907158248	0.929535959	0.533446070	0.28600843
$\ln(A_0-A_{600}/A_{240}-A_{600})$	0.463982715	1.359143372	1.022626382	0.552068582	0.79906620
$\ln(A_0-A_{600}/A_{300}-A_{600})$	0.908329611	2.611906341	1.537525331	0.671733086	0.91127819

Note: $A_{600} = A_{\infty}$

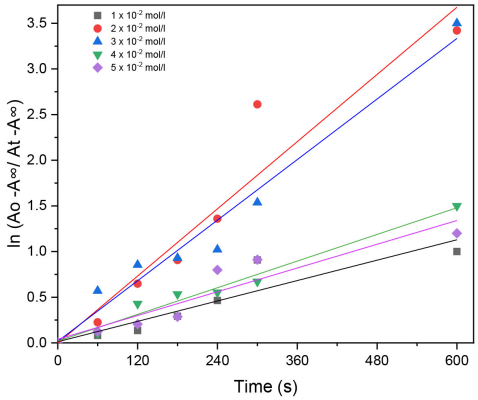

Figure 3: Influence of [mannose] on the redox reaction.

Table 6: Values of the rate constants of the redox reaction at various mannose concentration.

Concentration of mannose at mol/l	1×10^{-2}	2×10^{-2}	3×10^{-2}	4×10^{-2}	5×10^{-2}
The slope = k	0.00186	0.00613	0.00553	0.00243	0.00217

3.3.3 Influence of [H_2SO_4]

At the end of every 60 s, the absorbance was measured (Table 7). Plots of the ln Ao-A∞/At-A∞ versus time (Table 8, Figure 4) were likewise produced as straight lines, and the values of the rate constant were determined from the slopes of the plots (Table 9), suggesting that the rate of reaction rises with increasing H_2SO_4 concentration.

Table 7: Influence of [H_2SO_4] on the redox reaction.

t	1×10^{-1} mol/l	2×10^{-1} mol/l	3×10^{-1} mol/l	4×10^{-1} mol/l	5×10^{-1} mol/l
0	0.1665	0.1622	0.1742	0.1782	0.1721
60	0.1517	0.1500	0.1588	0.1721	0.1711
120	0.1483	0.1310	0.1525	0.1670	0.1701
180	0.1447	0.1038	0.1463	0.1652	0.1676
240	0.1435	0.0953	0.1410	0.1605	0.1653
300	0.1339	0.0742	0.1350	0.1499	0.1625
600	0.0839	0.0292	0.0920	0.1430	0.1610

Table 8: The values of ln Ao-A∞/At-A∞ of the redox reaction at various H_2SO_4 concentration.

ln A_o–A_∞/A_t–A_∞	1×10^{-1} mol/l	2×10^{-1} mol/l	3×10^{-1} mol/l	4×10^{-1} mol/l	5×10^{-1} mol/l
ln(A_0–A_{600}/A_{60}-A_{600})	0.197447486	0.096212843	0.207452222	0.190307908	0.094409684
ln(A_0–A_{600}/A_{120}–A_{600})	0.248896047	0.267339024	0.306511937	0.382992252	0.198670695
ln(A_0–A_{600}/A_{180}–A_{600})	0.306419892	0.578208621	0.414631075	0.460953794	0.519875459
ln(A_0–A_{600}/A_{240}–A_{600})	0.326354106	0.699180381	0.517335004	0.698845202	0.948330086
ln(A_0–A_{600}/A_{300}–A_{600})	0.501986675	1.083686638	0.647955186	1.629524671	2.00148

Note: $A_{600} = A_{\infty}$

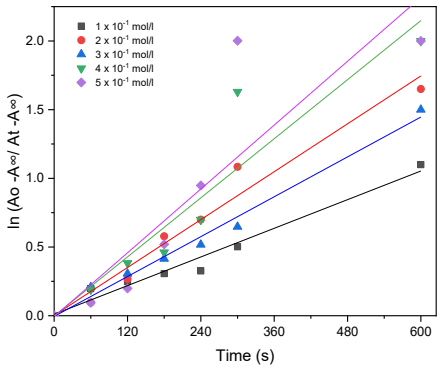

Figure 4: Influence of [H_2SO_4] on the redox reaction.

Table 9: Values of the rate constants of the redox reaction at various H_2SO_4 concentration.

Concentration of H_2SO_4 at mol/l	1×10^{-1}	2×10^{-1}	3×10^{-1}	4×10^{-1}	5×10^{-1}
The slope = k	0.00174	0.00291	0.00242	0.00358	0.00387

3.3.4 Influence of temperature

The curves of ln A_o-A_∞/A_t-A_∞ versus time (Table 10, Figure 5) were also plotted as straight lines, and the constant rate values were determined from the slope of the curves (Table 11), demonstrating that the response rate rises as the temperature rises. The activation energy (E_a) was derived from the slope of the curve $1/T \times 10^3$ and ln *k* (Table 12, Figure 6) according to the Arrhenius equation:[15]

$$K = \exp^{-Ea/RT} \quad \text{or} \quad In\ k = In\ A - \frac{E_a}{RT}$$

The following equations were used to compute the activation entropy change ($\Delta S^{\#}$) and activation free energy change ($\Delta G^{\#}$) (Table 13):

$$\Delta S^{\#} = 2.303R\left(\log A - \log \frac{RT}{Nh}\right)JK^{O}$$

$$\Delta G^{\#} = \Delta E_a - T\Delta S^{\#}\ KJ/mol$$

where R/N is Boltzmann's gas constant 1.3805×10^{-23} JK^{-1} and h plank's constant 6.62×10^{-34} J.S.

Table 10: Influence of temperature on the redox reaction.

T	A	Time (s)	A_o-A_∞	A_t-A_∞	A_o-A_∞/ A_t-A_∞	ln A_o-$_{A\infty}$/ A_t-A_∞
30°C	0.2437	0	0.0308	0.0308	1	0
	0.2409	60	0.0308	0.028	1.1	0.09531018
	0.2309	120	0.0308	0.018	1.711111111	0.537142932
	0.2244	180	0.0308	0.0115	2.67826087	0.985167655
	0.2202	240	0.0308	0.0073	4.219178082	1.439640342
	0.2143	300	0.0308	0.0014	22	3.091042453
	0.2129	600	0.0308	0	∞	3.30
35°C	0.2222	0	0.007	0.007	1	0
	0.221	60	0.007	0.0058	1.206896552	0.188052232
	0.2208	120	0.007	0.0056	1.25	0.223143551
	0.22	180	0.007	0.0048	1.458333333	0.377294231
	0.217	240	0.007	0.0018	3.888888889	1.358123484
	0.2161	300	0.007	0.0009	7.777777778	2.051270665
	0.2152	600	0.007	0	∞	2.20
40°C	0.2986	0	0.2929	0.2929	1	0
	0.2845	60	0.2929	0.2788	1.050573888	0.049336575
	0.2420	120	0.2929	0.2363	1.239526026	0.21472907
	0.2167	180	0.2929	0.211	1.388151659	0.32797312
	0.2111	240	0.2929	0.2054	1.425998053	0.354871956
	0.1680	300	0.2929	0.1623	1.804682686	0.590384779
	0.0057	600	0.2929	0	∞	0.87

(*continued on next page*)

Table 10: (*Continued*)

T	A	Time (s)	A_o-A_∞	A_t-A_∞	A_o-A_∞/ A_t-A_∞	ln A_o-$_{A\infty}$/ A_t-A_∞
45°C	0.2260	0	0.0371	0.0371	1	0
	0.2178	60	0.0371	0.0289	1.283737024	0.249775374
	0.2148	120	0.0371	0.0259	1.432432432	0.359374001
	0.2147	180	0.0371	0.0258	1.437984496	0.363242478
	0.2100	240	0.0371	0.0211	1.758293839	0.564343929
	0.1983	300	0.0371	0.0094	3.946808511	1.37290728
	0.1889	600	0.0371	0	∞	1.70
50°C	0.2202	0	0.0213	0.0213	1	0
	0.2151	60	0.0213	0.0162	1.314814815	0.27369583
	0.2143	120	0.0213	0.0154	1.383116883	0.324339563
	0.2123	180	0.0213	0.0134	1.589552239	0.463452366
	0.2047	240	0.0213	0.0058	3.672413793	1.300849155
	0.2035	300	0.0213	0.0046	4.630434783	1.532650769
	0.1989	600	0.0213	0	∞	2.30

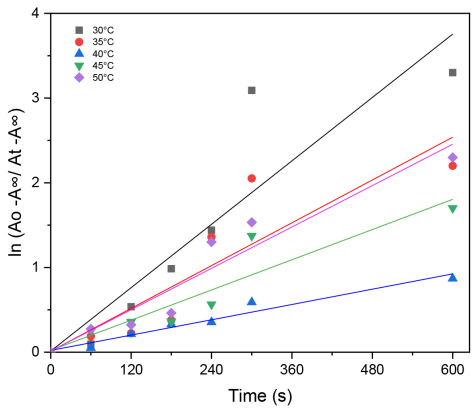

Figure 5: The influence of temperature on the redox reaction.

Table 11: The values of the rate constant of the redox reaction at different temperatures.

Temperature °C	30	35	40	45	50
The slope = k	0.00324	0.00421	0.00651	0.01097	0.01307

Table 12: Values of $1/T \times 10^3$ and ln k.

T^oK	10^3 1/T	10^3 k sec^{-1}	ln k
303	3.300	3.24	–5.732
308	3.247	4.21	–5.470
313	3.195	6.51	–5.034
318	3.145	10.97	–4.512
323	3.096	13.07	–4.337

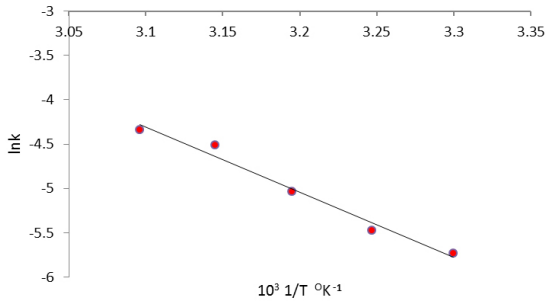

Figure 6: Plot of ln k versus 1/T for mannose – manganes(vii) reaction.

Table 13: Thermodynamic parameters for the redox reaction at different temperatures.

Physical parameter	Found				
Activation energy (E_a) in $KJ.mol^{-1}$	61.1				
Frequency factor (A) in sec^{-1}	10.52×10^5				
Free energy change (ΔG) in $KJ.mol^{-1}$ at different temperatures	30°	35°	40°	45°	50°
	27.77	28.27	28.77	29.27	29.77
Entropy change (ΔS) in $J.K^{-1}$ at different temperatures	30°	35°	40°	45°	50°
	–91.45	–91.59	–91.72	–91.85	–91.98

3.3.5 Mechanism and rate law of the reaction

We propose the following simplified mechanism to explain the pathway of mannose oxidation by Mn^{+7} in an acidic medium:

$$mannose + Mn^{+7} + H^{+} \underset{k_2}{\overset{k_1}{\rightleftharpoons}} \underset{Complex}{[mannose..... Mn^{+7}]}$$

$$\underset{Complex}{[Mannose..... Mn^{+7}]} \xrightarrow[\text{slow}]{K_3} [Product]$$

Where k_1 and k_2 represent the rates in the forward and reverse directions, respectively and k_3 represents the rate at which the product is formed. The complex creation rate is provided as follows:

$$d\ \frac{[Complex]}{dt} = k_1\,[mannose][\,Mn^{+7}\,] - [k_2 - k_3\,][Complex] \tag{1}$$

At a steady state,

$$d\ \frac{[Complex]}{dt} = 0 \tag{2}$$

From equation (1) and (2) the concentration of the complex results to be:

$$[Complex] = \frac{k_1[mannose][Mn^{+7}]}{k_2 + k_3} \tag{3}$$

In a steady state, the rate of disappearance of Mn^{+7} can be:

$$-d\frac{[Mn^{+7}]}{dt} = k_3[Complex] \tag{4}$$

$$-d\frac{[Mn^{+7}]}{dt} = \frac{k_3k_1[mannose][Mn^{+7}]}{k_2 + k_3} \tag{5}$$

Now the total $[Mn^{+7}]$ may be considered as:

$$[Mn^{+7}]_T = [MnO^{+7}] + [Complex] \tag{6}$$

In putting the value of Complex:

$$[Mn^{+7}]_T = [MnO^{+7}] + \frac{k_1[mannose][Mn^{+7}]}{k_2 + k_3} \tag{7}$$

From equation (7), the value of $[Mn^{+7}]$ comes out :

$$[Mn^{+7}] = \frac{(k_2 + k_3)[Mn^{+7}]_T}{(k_2 + k_3) + k_1[Mannose]} \tag{8}$$

So the final rate law from (5) to (8):

$$-d\ \frac{[Mn^{+7}]}{dt} = \frac{k_3k_1[mannose](k_2 + k_3)[Mn^{+7}]_T}{\{k_2 + k_3 + k_1[mannose]\}(k_2 + k_3)} \tag{9}$$

$$= \frac{k_3 k_1 [mannose][Mn^{+7}]_T}{\{(k_2 + k_3) + k_1 [mannose]\}} \quad (10)$$

This article follows the condition that: $(k_2 + k_3) > k_1 [mannose]$. Therefore, the above equations (9) and (10) reduce to,

$$\frac{-d[Mn^{+7}]}{dt} = \frac{k_3 k_1 [mannose][Mn^{+7}]_T}{(k_2 + k_3)} = k[mannose][Mn^{+7}]_T \quad (11)$$

where,

$$k = \frac{k_3 k_1}{(k_2 + k_3)}$$

The above equation shows first-order kinetics concerning the concentration of mannose and permanganate ions.

4. CONCLUSION

$KMnO_4$ (the source of Mn^{+7} in this study) is very reactive under certain conditions. Under strongly acidic conditions, manganese is reduced from (Mn^{+7}) to (Mn^{+2}), while under weakly acidic conditions it is reduced to Mn^{+4}. The following reaction was observed:

$$MnO_4^- + 4H^+ + 3e^- \longrightarrow MnO_2 + H_2O$$
$$MnO_4^- + 8H^+ + 5e^- \longrightarrow Mn^{+2} + 4H_2O$$

Based on stoichiometric studies, it is easy to determine that MnO_4^- is the active, reactive oxidising species in an acidic media that reacts with H^+ ions to produce permanganic acid.

$$H^+ + MnO_4^- \rightleftharpoons HMnO_4$$

This highly reactive inorganic acid, permanganic acid, oxidises the sugar mannose to produce an unstable intermediate complex, which then converts to aldehyde hydrate. Frequently, this aldehyde hydrate transforms into the equivalent carboxylic acid when it combines with MnO_3^- species.

The present study is based on the oxidative property of Mn^{+7} in an acidic medium with organic reducing mannose sugar. Two primary products, an arabinonic acid, a formic acid and the corresponding acids of mannose have been discovered.

$$C_6H_{12}O_6 + 2MnO_4^- \xrightarrow{H^+} C_5H_{10}O_5 + HCOOH + 2MnO_3^-$$

These products might result from the oxidation of $KMnO_4$ into two different species in an acidic media. The respective acid of mannose due to the generation of reactive oxygen species in presence of an acid, the corresponding formic and arabinonic acids result from the breakdown of the C-C bond by the reactive species of MnO_4^-.

According to the proposed mechanism, it was discovered that the uncatalysed reaction of Mn^{+7}/H^+ ions with mannose sugar molecule exhibits first-order kinetics concerning mannose and permanganate ion concentration, and the linear dependence of rate is observed when the acidity of the medium increases (Table 9).

Findings also showed that the reaction rate was enhanced by 3×10^{-4} m of $KMnO_4$ concentration (Table 3) and the oxidation with $KMnO_4$ was found to be faster using 2×10^{-2} m of Mannose (Table 6) and 5×10^{-1} m of H_2SO_4 (Table 9).

Two parameters—one indicating the intercept and the other the slope of the straight line—are often included to characterise the temperature dependence characteristic of the reaction analytically. The intercept of the line (Figure 6) provided the frequency factor (in s^{-1}) for the parameter A, which was determined to be 10.52×10^5. The line's slope revealed that the parameter E_a, the activation energy, equals 61.1 KJ.mol^{-1}. The activation's free energy change ($\Delta G^{\#}$) and entropy change ($\Delta S^{\#}$) were also estimated. Results are shown in Table 13.

A negative activation entropy value indicates the existence of highly solvated transition intermediate states, while sluggish kinetics is indicated by a positive activation energy value. The negative value of $\Delta SG^{\#}$, which denotes the intermediate solvated state, supports the positive value of the activation free energy, which implies a substantial electrostatic contact between the solute and the solvent.

5. ACKNOWLEDGEMENTS

The author extends his appreciation to the department of chemistry, Faculty of Science at Northern Border University, Arar, KSA where these investigations were carried out.

6. REFERENCES

1. Jain, J. L. et al. (2010). *Fundamentals of biochemistry.* Ram Nagar, New Delhi: S. Chand and Company LTD, 73.
2. Singh, A. K. et al. (1998). Kinetics and mechanism of Pd(II) catalysed oxidation of D-arabinose, D-xylose and D-galactose by *N*-bromosuccinimide in acidic solution. *Carbohydr. Res.*, 314 (3–4), 157–160. https://doi.org/10.1016/S0008-6215(98)00322-X
3. Tripathi, R. & Upadhyay, S. K. (2004). Kinetics of oxidation of reducing sugars by catalytic amount of osmium(VIII) in presence of periodate. *Int. J. Chem. Kinet.*, 36(8), 441–448. https://doi.org/10.1002/kin.20017
4. Odebunmi, E. O. et al. (2009). Kinetics and mechanism of oxidation of D-xylose and L-arabinose by chromium(VI) ions in perchloric acid medium. *Int. J. Biol. Chem. Sci.*, 3(2), 178–185. https://doi.org/10.4314/ijbcs.v3i2.44485
5. Odebunmi, E. O. et al. (1999). The kinetics and mechanism of oxidation of D-glucose, and D-sorbitol by $KMnO_4$ and hexachloroiridate (IV). *Nigerian J. Sci.*, 33, 133–143.
6. Albert Lehninger, L. (2003). *Biochemistry*, 2nd ed. New York: Worth Publication, 249.
7. Eric Conn, E. et al. (2004). *Outlines of Biochemistry*, 5th ed. New York: John Wiley and Sons, 25.
8. Azmat, R. et al. (2012). Kinetics and mechanisms of oxidation of D-fructose and D-lactose by permanganate ion in acidic medium. *Nat. Sci.*, 4(7), 466–478. https://doi.org/10.4236/ns.2012.47063
9. Dash, S. et al. (2009). Oxidation by permanganate: Synthetic and mechanistic aspects. *Tetrahedron*, 65, 707–739. https://doi.org/10.1016/j.tet.2008.10.038
10. Gupta, K. K. S. et al. (2000). Reactivities of some aldoses and aldosamines towards potassium bromate in hydrochloric acid medium. *J. Indi. Chem. Soc.*, 77, 152–156.
11. Odebunmi, E. O. et al. (2006). Kinetics of oxidation of fructose, sucrose and maltose by potassium permanganate in $NaHCO_3$/NaOH buffer and Iridium(IV) complex in sodium acetate/acetic acid buffer. *Int. J. Chem.*, 16, 167–176.
12. Krishna, K.V. & Rao, P. J. P. (1995). Kinetics and mecha-nism of oxidation of some reducing sugars by diperioda-toargentate(III) in alkaline medium. *Transit. Met. Chem.*, 20, 344–346. https://doi.org/10.1007/BF00139125
13. Azmat, R. et al. (2008). Kinetics and mechanism of oxidation of D-galactose and D-maltose with potassium permanganate in acidic medium by spectrophotometry. *Asian J. Chem.*, 20(2), 829–837.
14. Abdel-Hamid, M. I. et al. (2003). Kinetics and mechanism of permanganate oxidation of pectin polysaccharide in acid perchlorate media. *Euro. Polym. J.*, 39, 381–387. https://doi.org/10.1016/S0014-3057(02)00217-3
15. Reidies, A. H. (2002). *Manganese compounds in Ull-mann's Encyclopedia of industrial chemistry*. Weinheim: Wiley-VCH.

16. Sen Gupta, K. K. S. et al. (1983). Kinetics of Oxidation of D-glucose by Hexachloroiridate (IV) and Terchloroaurate (III). *Carbohydr. Res.*, 117, 81. https://doi.org/10.1016/0008-6215(83)88076-8
17. Odebunmi E. O. & Owalude S. O. (2005). Kinetics and mechanism of oxidation of sugars by chromium (VI) in perchloric acid medium. *J. Chem. Soc. Nigeria.*, 30, 187.
18. Tripathi, R. & Upadhyay, S. K. (2004). Kinetics of oxidation of reducing sugars by catalytic amount of osmium(VIII) in presence of periodate. *Intern. J. Chem. Kinetics*, 36, 441. https://doi.org/10.1002/kin.20017
19. Abualreish, M. J. A. (2018). The effect of surface on the redox reaction between D (+) glucose and persulphate ion and evaluation of the reaction's activation energy. *Res. J. Chem. Environ.*, 22(7), 12–17.
20. Abualreish, M. J. A. (2021). Evaluation of thermodynamic properties and the effect of surface on the uncatalyzed thermal decomposition of potassium peroxydisulphate in neutral solution. *Res. J. Chem. Environ.*, 25(3), 142–147.